

Modeling sea fog on the U.S. California coast during a hot spell event

Darko Koračin¹, Dale F. Leipper[†]¹ and John M. Lewis^{1,2}

¹ Desert Research Institute, Reno, Nevada, U.S.

² National Oceanic and Atmospheric Administration, Severe Storms Laboratory, Norman, Oklahoma, U.S.

Received 24 September 2004, in final form 27 June 2005

The occurrence of sea fog along the U.S. Pacific Coast in summer is frequently associated with the movement of a high pressure system from the eastern Pacific to the land. Subsequently there is strong heating of the land over several days or more and development of »hot spells« and offshore flows in the coastal region preceding sea fog formation. This study focuses on modeling the formation and evolution of sea fog in response to interaction between the warm and dry offshore flows and the cool and moist marine atmospheric boundary layer. Simulation results support a conceptual model of fog formation and evolution based on physical processes initiated by offshore flows that efficiently lower the marine inversion near the sea surface. In spite of the warm and dry advection, fog formed in the shallow, near-surface marine layer capped by a strong temperature inversion of 10 °C or more and a hot-air layer above the inversion. Prior to sea fog formation, negative surface heat flux initiates cooling and condensation, while the surface moisture flux contributes to increased humidity and turbulence within the surface layer. The dryness of the hot-air layer overlying the shallow and moist marine layer triggers enhanced radiative cooling at the marine layer top and facilitates the marine layer's saturation. The thin cloud forms, rapidly propagates downward, and transforms into fog. As soon as the fog is formed, longwave radiative cooling at its top generates turbulent mixing and the growth of the fog as a mixed layer. Due to the fog-top radiative cooling, the fog layer is initially colder than the underlying surface. In the later stage of the fog evolution, continuous mixing of the cool and moist near-surface air with the dry and warm layer above the inversion during the fog growth generally curtails turbulence. This process elevates the lifting condensation level and can lead to sea fog dissipation or generation of stratus.

Keywords: Air-sea interaction, longwave radiation cooling, marine atmospheric boundary layer, numerical simulations, offshore flows, offshore fog, U.S. West Coast.

[†] Born 1914. – Deceased 2004.

1. Introduction

Modeling studies of fog over land have benefited from relatively abundant measurements and this has led to better understanding of the phenomenon. In contrast, sea fog and the main determinants of its formation are poorly understood. Sea fog is relatively frequent along the West Coast of the United States – nevertheless; there is significant variability by season and location (Filonczuk et al., 1995; Lewis, 2004). Leipper (1994) and Lewis et al. (2003) have indicated that forecasting of sea fog along the California coast is a complicated task due to the delicate interplay of physical processes, coastal topography, and synoptic forcing as well as the scarcity of routine offshore observations. Conditions similar to those on the California coast – with offshore flows crossing coastal mountains and a cool sea surface – occur in other areas including the coastal regions of Ecuador, Peru, Chile, western Morocco, and southwest Africa where similar coastal upwelling exists (see, *e.g.*, Leipper, 1994).

Figure 1 shows the spatial distribution of sea fog frequency along the California coast. The data are extracted from Filonczuk et al. (1995) and discussed by Lewis et al. (2003; 2004). The Y-axis on each of the sub-regional figures indicates the ratio of hours when fog was observed to the total number of observation hours. Two main characteristics can be inferred from Fig. 1. The histograms suggest that the maximum occurrence of coastal sea fog is generally in the summer and fall. Note, however, that the offshore region does not exhibit the same relative frequency. The number of sea fog cases is greatest near the coast and decreases as one moves further offshore. Consequently, it is important to understand the properties of the atmospheric flows near the coastline and air-sea interaction processes relevant to sea fog formation.

A common type of spring-summer sea fog occurs along the U.S. West Coast following the movement of a high pressure system from the eastern Pacific to land. These synoptic conditions induce strong heating inland that can propagate to the coast. The pressure gradient directed from the land to the sea initiates warm and dry offshore flows over large sections of the coast. These conditions are referred to as »Hot Spells« (Leipper and Koračin, 1998; hereafter LK98).

The formation of sea fog in the presence of the warm and dry conditions remains poorly understood. Beginning with pioneering studies by Byers (1930), Petterssen (1938), and Leipper (1948), several explanations have been offered for the formation and evolution of coastal fog on the U.S. west coast. Byers (1930) and Hsu (1988), among others, claim that sea fog forms when the onshore flows traverse cool and upwelled waters. On the other hand, Leipper (1948; 1994; and 1995) hypothesized that fog is formed when the offshore warm and dry flow replaces the near-surface marine atmospheric layer. In this explanation, the very shallow layer (on the order of a few meters deep)

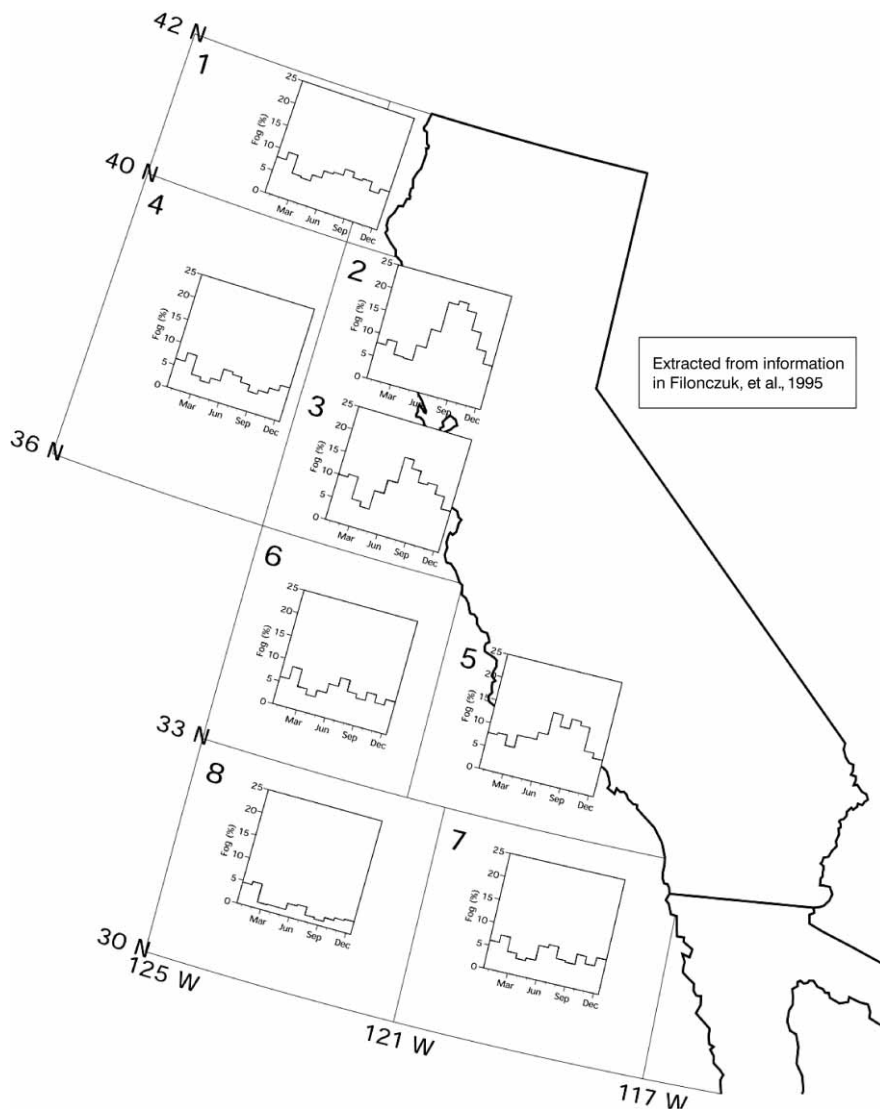


Figure 1. Relative monthly frequencies (in percentages) of sea fog hours along the California coast by regions for the period 1949–1991. The data are extracted from Filonczuk et al. (1995). The plot is reproduced from Lewis et al. (2003; and 2004). See above text for more details.

adjacent to the sea surface becomes saturated. Once a shallow fog is formed, the mixing generated by radiative processes causes growth of the fog as a mixed layer. Petterssen’s (1938) view stressed the importance of buoyancy in warm-sea conditions that leads to condensation in the turbulent marine layer.

With the benefit of field work in the post – WW II era, the processes that lead to sea fog have been clarified. In particular, field work in the 1970s by the Naval Postgraduate School and the Cornell Aeronautical Laboratory (CALSPAN) (Pilié et al., 1979) spurred numerical experimentation (Oliver et al., 1978). Despite the availability of those special offshore observations and associated computer modeling, a full understanding of the processes is elusive. We elaborate by focusing on the formation of sea fog by stratus lowering or stratus deepening. In Oliver et al. (1978), numerical experiments with a one-dimensional turbulence/radiation transfer model led investigators to believe that sea fog formed as a result of radiative cooling at the stratus top and an associated downward vertical extension of the cloud through microphysical processes – a link between microphysical droplet formation and the radiative cooling. On the other hand, the study by Koračin et al. (2001) indicated that stratus lowering to produce sea fog hinged on a combination of negative buoyancy in response to radiative cooling atop the stratus in conjunction with buoyancy at the air-sea interface as the air column experienced long over-water trajectories. Although the processes described by Oliver et al. (1978) and Koračin et al. (2001) are different, it is quite possible that they are operative in separate synoptic situations. To the eye, the formation of sea fog from each of these separate processes would likely appear similar.

The current study is an outgrowth of earlier work in LK98. In that study, we discussed the importance of hot-spell events in initiating fog formation over the ocean in a coastal region. We argued that the cooling of the hot air layer over a much cooler sea can lead to fog formation. In these situations, the temperature difference between the hot-air layer and the sea is generally 5–15 °C. Once condensation commences, radiative effects initiate mixing and growth of the fog layer.

The triggering mechanism for the condensation processes is still puzzling, and this justifies further exploration. Observations have been made which show fog forming at the sea surface and growing upward as a mixed layer until a critical depth of several hundred meters is reached. In order to simulate fog formation initiated at the sea surface, we need to fully understand the processes occurring at the surface and the critical conditions for the initial fog development. In the absence of detailed measurements at the sea surface and without a solid explanation for this initial formation and evolution leading to the equilibrium state, we will base our modeling study on a characteristic case of hot spell on the U.S. Pacific coast and focus on sensitivity tests of initial and boundary conditions essential to the evolution of fog.

In order to investigate the particular roles of the different processes influencing fog in the aftermath of hot-spell events, we performed a numerical experiment. The numerical experiment investigates the importance of turbulence transfer and radiation processes in governing the growth of a fog layer. The main focus is on understanding the role of the particular initial and boundary conditions in fog prediction. We selected a one-dimensional turbu-

lence-closure model as an investigative tool. Although one-dimensional models lack spatial variability and advective processes, they allow for high vertical resolution and make feasible sensitivity tests of all significant initial and boundary conditions that influence the prediction of certain weather phenomena. They are often used for baseline studies of basic physical processes influencing simulation results. The knowledge gained from these baseline studies is then used in two- and three-dimensional numerical studies. We first constructed initial conditions for the baseline simulation using a conceptual model and data from a hot-spell event on the U.S. California coast (LK98). The importance of sufficient vertical resolution on the simulated fog evolution was then investigated using a wide range of vertical resolutions (45 to 180 points) within the first 1200 m. Third, sensitivity tests of critical boundary and initial conditions for fog formation were performed. In particular, these tests include variations of the sea-surface temperature (SST), inversion characteristics, and properties of the near-surface and hot-air layers.

2. Hot spells

Figure 2 shows the basic components of Leipper's conceptual model of sea fog formation during a hot-spell event in response to the synoptic setup and the development of offshore flows. This event is characterized by a period of unusually warm weather and associated offshore flow of hot air, which experiences further heating via adiabatic descent of air along trajectories from land to sea. The near-surface temperature of the air is 5–15 °C greater than the temperature of the adjacent sea surface over the coastal waters. Leipper has advocated the importance of this phenomenon and its influence on U.S. Pacific Coast weather for more than half a century (Leipper, 1948, 1994; Filonczuk, 1995 (Appendix C); LK98). These hot-spell events appear to significantly influence coastal weather such as sea fog (Leipper, 1994), the Catalina Eddy (Rosenthal, 1974), and wind surges and coastally-trapped disturbances (CTD) (Nuss et al., 2000).

It is important to recognize that the differences in large-scale factors leading to sea or coastal fog are often subtle. For example, the mechanisms advocated by Leipper rely on the land-to-sea flow where the warm and dry air replaces the marine-layer air – in essence, a forced movement of the marine air such that the land-based air displaces it seaward. In contrast to this mechanism, it seems reasonable to expect that there are situations where the land-based air mass rides up over the marine layer – *i.e.*, it does not displace the marine layer air next to the coast. The case studied by Koraćin et al. (2001) appears to follow this latter scenario. We suspect that both of these processes can be operative in different cases.

There has been a history of using one-dimensional turbulence-closure models to investigate marine and lake boundary-layer processes (*e.g.*, Stage and Businger, 1981; Koraćin and Rogers, 1990; Burk and Thompson, 1992;

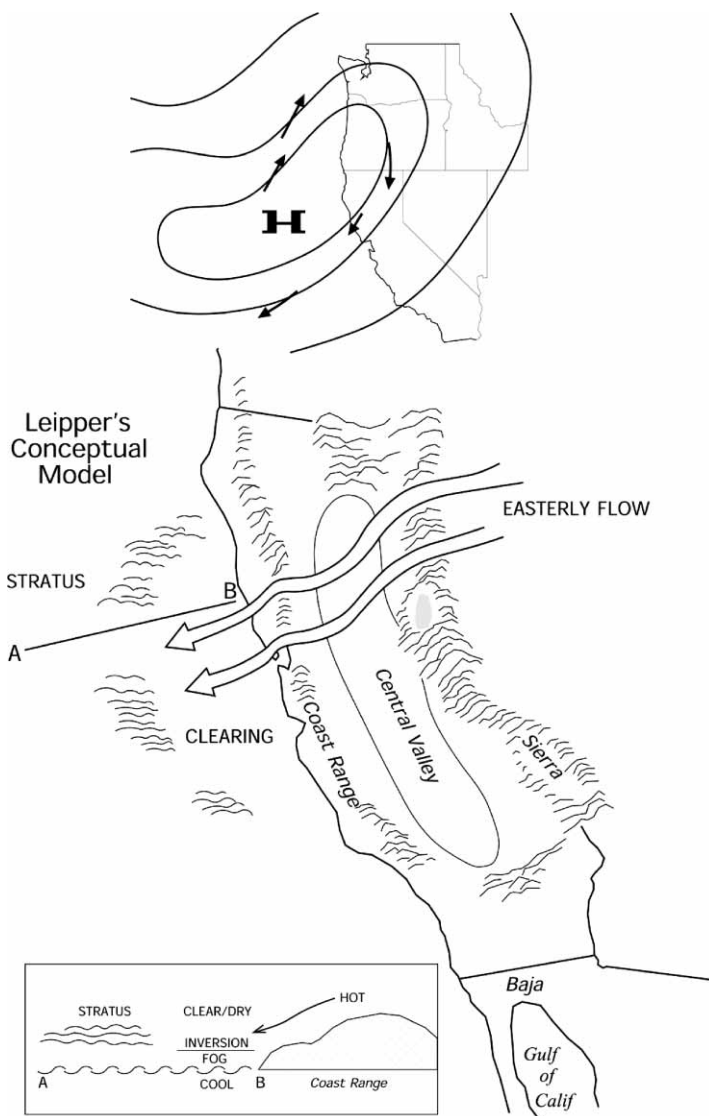


Figure 2. A schematic of Leipper's conceptual model of sea fog formation during a hot-spell event. The upper portion of the diagram shows the surface airflows associated with the position of the Pacific anticyclone. The lower portion of the diagram shows the relative position of clear air, fog, and stratus relative to the coastline. The plot is reproduced from Lewis et al. (2003; and 2004). See text for further details.

Rogers and Koračin, 1992; Tjernström and Koračin, 1995; Smith and Kao, 1996; Koračin et al., 2001). Justification for the use of these simpler models rests on the desire to more clearly understand physical processes – *i.e.*, the

models have fewer elements in the control vector and interplay between physical processes are often easier to unravel compared to the multi-dimension models with coarser resolution. In particular, the fine-scale vertical resolution is often a central advantage for these models. In Koračin et al. (2001), the fine scale vertical resolution of 3–10 m made it possible to accurately quantify the net radiative fluxes that were key to the fog formation. Recently, Koračin et al. (2005) used 3D numerical simulations to develop a qualitative and quantitative understanding of the modification of the cloudy marine layer along long over-water trajectories relevant to the formation of sea fog. They identified the roles of radiational cooling, advection, surface fluxes, and entrainment on the fog formation, evolution and eventual dissipation.

In regard to this particular application, *i.e.*, study of the hot spell fog, we are justified in using an Eulerian view since the environment in which the fog forms shows little if any influence of advection, *i.e.*, we are interested in changes in the marine layer when the hot-air layer is already located at the site where fog can form. The large-scale synoptic flow establishes a strong inversion off the coast and the flow of low-level air is from land to sea. The horizontal movement of the slabs of air, generally from east to west near the coastline, is not associated with changes in lower boundary conditions (changes in SST) or with differing structures of air adjoining the sea. This, at least, is the case for distances on the order of 50–100 km from the coast. The CTDs, which typically move from south to north along the coast, are more likely linked to changing boundary conditions (colder SSTs to the north). This is also the case for the fog in association with long over-water trajectories (from north to south) of air that was studied by Koračin et al. (2001; 2005).

3. Synoptic characteristics of a hot-spell event of 16–17 May 1997

A coastally trapped disturbance moved from the Southern California Bight up through San Francisco between 1800 UTC on 16 May and 1800 UTC on 17 May 1997. The visible imagery from the GOES satellite shows its position as the front approaches San Francisco (Fig. 3). As can be seen in Fig. 4, the dominant synoptic features associated with this fog event are large-scale cyclonic circulations in the eastern Pacific Ocean and over southwestern Canada. Between these systems there exists a ridging pattern, especially in evidence at the lower levels (850 and 1000 mb). It is the protrusion of this ridge into the Pacific Northwest that is the primary signature of the hot-spell event. In some cases, an anticyclone moves onshore and can persist for several days (see Koračin et al., 2001). In this case, the anticyclonic center remains offshore and the ridge is more transitory. These weaker systems are associated with minimal subsidence (approximately $0.5\text{--}1.0\text{ cm s}^{-1}$) at the 850–700 mb levels. The upper-air sounding at Oakland at 1200 UTC on 17 May 1997 (figure not shown) indicated an offshore flow at the 850 mb level.

Data from the buoys offshore of California showed abrupt changes of wind direction as the CTD passed these stations. Typically, northwesterly flow at the surface abruptly changed to southerly flow. The time series of wind speed, wind direction, and air temperature from the buoy off San Francisco Bay is shown in Fig. 5. Here we note the abrupt shift of wind at 1000 UTC, 17 May 1997, and an associated sudden rise in air temperature. After a lull in wind speed at the time of the wind shift, this speed increases gradually, but this is air that comes from the land (easterly flow). The data from the buoy off San Francisco (SFO) exhibits an easterly flow after the surge passage, whereas the buoys located further south exhibited a shift to a more southerly wind. The easterly flow at SFO appears to be related to the intrusion of the ridge that extended southward to the San Francisco area, but not to points further south. On the other hand, the CTD did not extend northward beyond the San Francisco Bay. Thus, the synoptic setting with the hot spell near San Francisco favored the low-level offshore flow over this region in conjunction with the intrusion of the CTD from the south.

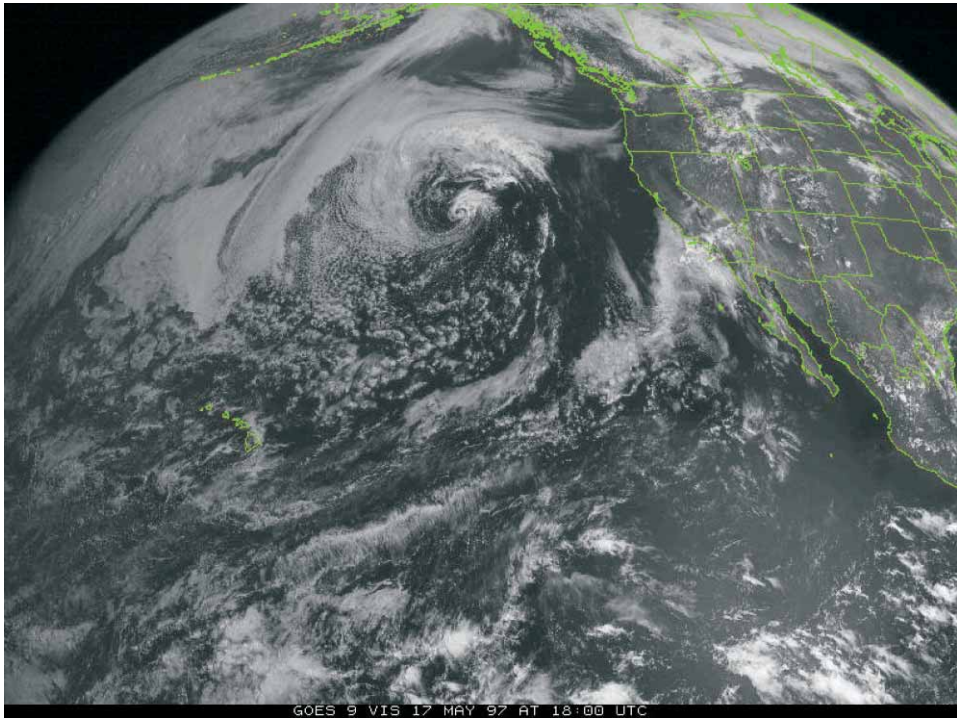


Figure 3. Visible satellite imagery from the geostationary satellite GOES at 1800 UTC, 17 May 1997. The narrow tongue of stratus cloud abuts the California coastline and is associated with the northward propagating coastally trapped disturbance (CTD).

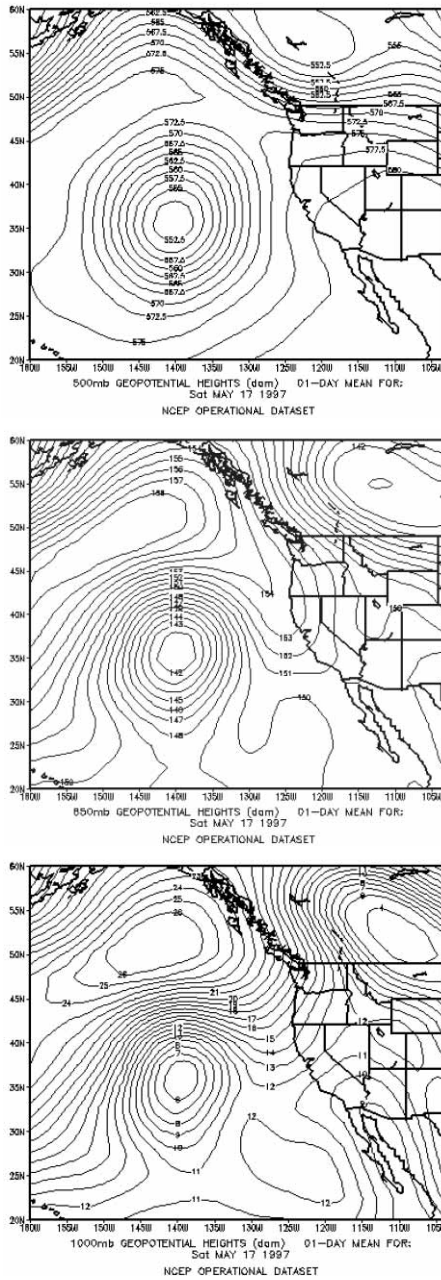


Figure 4. Large-scale synoptic patterns at 500 mb (top panel), 850 mb (middle panel), and 1000 mb (bottom panel) over the Pacific Ocean and western United States. The semi-permanent cyclonic pattern over the ocean exhibited retrogression over the preceding 24-hr period and began to disconnect from the westerlies over British Columbia.

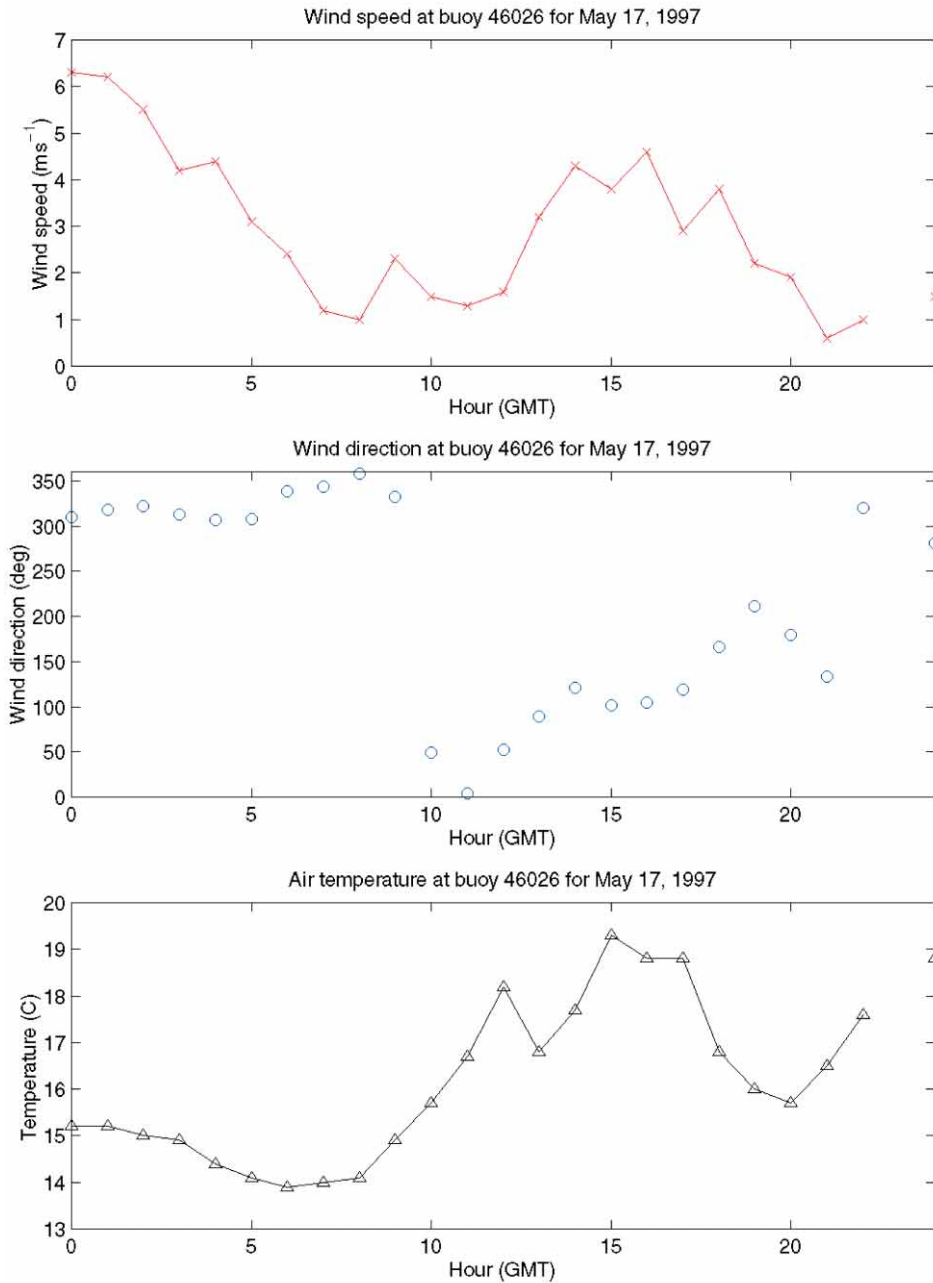


Figure 5. Time series of the wind speed (m s^{-1}) and wind direction ($^{\circ}$) (at 5 m height), and air temperature ($^{\circ}\text{C}$) (at 3.5 m height) observed by the buoy near San Francisco Bay on 17 May 1997.

4. Numerical Experiment

We applied a one-dimensional, higher-order, turbulence-closure model to an idealized case of a hot-spell event. The model used in this study was fully described by Koraćin (1989), Koraćin and Rogers (1990), Rogers and Koraćin (1992), Leipper and Koraćin (1998), and Koraćin et al. (2001). The model consists of prognostic equations for horizontal wind components, liquid water potential temperature, mixing ratio of total water, and the turbulence kinetic energy (TKE).

The numerical experiment consisted of a baseline simulation and a series of sensitivity tests focused on the influence of critical thermodynamical and dynamical parameters on the formation and evolution of sea fog. The baseline setup used the initial and boundary conditions from the hot-spell event that occurred on 16–17 May 1997 that is described in Section 3. Sensitivity tests were selected to investigate the particular roles of sea surface temperature, increased temperature and reduced moisture in the hot-air layer, the strength of the inversion imposed by the hot spell, and the source of mixing in the near-surface layer necessary to have fog penetrate the hot-air layer. Sensitivity tests also included random perturbations in the surface wind speed and wind stress (Koraćin et al., 2004) to account for the influence of surface ocean waves that is not treated in the model. In addition, the perturbations reflect the uncertainty in determining the wind speed and its unsteadiness due to turbulence processes.

4.1. Baseline simulation

Idealized conditions representative of the intrusion of hot spells over coastal water were constructed for the baseline simulation using the hot spell event which occurred on the U.S. California coast on 17 May 1997 described in Section 2. Three vertical layers were defined for initial conditions:

- Shallow, near-surface marine layer in the first 100 meters: this air layer is in balance with the sea surface and is consequently well mixed with a potential temperature of 13.2 °C. These layers are characterized by light onshore western and northwestern winds (Leipper and Koraćin, 1998). The mixing ratio of water vapor is constant with height (10 g kg⁻¹). The assumed high relative humidity in the marine layer represents the effect of moisture accumulation in the very shallow marine layer capped by the strong inversion. It should be noticed that high relative humidity in the marine layer does not necessarily guarantee fog formation (Filonczuk et al., 1995).
- Hot-air layer: this layer is created by the hot spell. It extends from the top of the shallow, near-surface marine layer to the usual height of the elevated marine inversion (approximately 400 m). This layer is potentially 10 °C warmer; the mixing ratio of the water vapor drops by 4 g

kg^{-1} from the top of the shallow, near-surface layer to the top of the hot-air layer. Offshore winds are northeasterly in this layer. A marine layer temperature inversion of about $10\text{ }^{\circ}\text{C}$ is frequently observed over the U.S. West Coast waters (Koračin et al., 2001 and 2005; Lewis et al., 2003).

- Layer above the elevated inversion: a potential temperature gradient of $3.5\text{ }^{\circ}\text{C km}^{-1}$ above the elevated inversion is assumed from the top of the hot-air layer to the top of the domain. The water vapor mixing ratio is assumed to drop by 1 g kg^{-1} from the top of the hot air layer to the top of the domain (1200 m). Northwestern onshore winds are assumed in this layer.
- We assume a weak subsidence based on earlier experience with these offshore flows (see Koračin et al., 2001; Lewis et al., 2004). With a strong high pressure ridge inland, the subsidence can reach $3\text{--}4\text{ cm s}^{-1}$ at the coast, whereas with a weaker system such as this one, the subsidence rates are typically below 1 cm s^{-1} (see non-fog case in Lewis et al., 2003).

Figure 6 shows the initial vertical profiles of the potential temperature, the mixing ratio of water vapor, and the U and V wind velocity components, which are based on the Leipper and Koračin (1998) study. In this wind profile, we note a northwesterly flow in the lowest levels (below 30–40 m), but northeasterly flow above. This reflects the »two-fluid« system, with marine layer at the lower levels and the hot/dry land-based air above. This state is representative of the pre-fog conditions as shown before 1000 UTC in Fig. 5. When the marine-layer flow weakens as shown in Fig. 5 (top panel), that facilitates the penetration of the northeasterly flow to lower levels.

Sea surface temperature was held at $14\text{ }^{\circ}\text{C}$ which is representative of the Monterey coastal waters. The simulation was performed for 168 hours (7 days). Although it is likely that fog would be disturbed by the synoptic system within this time period, the long duration of the simulation provided information about whether or not the system would reach an equilibrium state and maintain fog.

A stratus layer with a base near the sea surface formed within the first hour of the simulation. This layer deepened downward due to cooling and continuous moisture flux and then transformed into fog within the first two hours. Longwave radiative cooling at the cloud top initiated turbulent mixing and overall cooling of the near-surface layer. The greatest cooling of the mixed layer (approximately $1.5\text{ }^{\circ}\text{C}$) occurred within the first day (Fig. 7). The fog became colder than the sea surface and consequently initiated a positive surface heat flux. The longwave cooling was nearly balanced by the heating due to the surface heat flux. According to our simulations, the cooling was also partially reduced by continuous mixing of the cool and moist layer with the hot and dry layer above as well as with the released latent heat. The sim-

ulations clearly show that the fog grew as a mixed layer, reaching 180 m in depth after 6 days. At that time the fog growth is reduced in response to the balance of fog-top radiative cooling, the turbulence that generated the fog growth, and entrainment of warm and dry air.

Figure 8 shows vertical profiles of the mixing ratio of liquid water for every 24 hours of the simulation. It should be noted that the profiles closely resemble adiabatic profiles. A maximum liquid-water mixing ratio of 0.38 g kg^{-1} was reached on day 5 and became less on later days due to entrained warm and dry air during the fog growth. Turbulent mixing maintained the mixed layer and supported continued vertical growth of the mixed layer into the hot-air layer. The TKE was fairly high and relatively uniform with height (Fig. 9). It had a maximum near the surface due to surface fluxes. The TKE decreased with time because of a general increase in stability due to mixing of the cool, near-surface layer with the hot-air layer. The fog grew as a mixed layer vertically approximately 20–30 m per day. The maximum liquid water mixing ratio was reduced toward the end of the simulation due to the previously mentioned effect of the cool and moist near-surface layer mixing with the hot and dry layer above. During the seventh day, the fog approached a depth of 200 m. The simulation indicated that an equilibrium state was not reached in the seven day period.

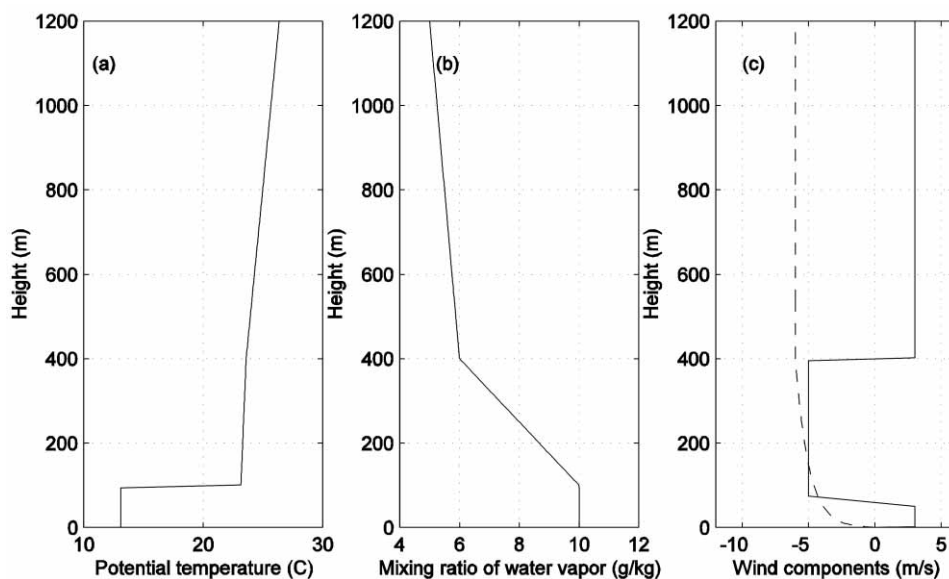


Figure 6. Initial profiles of the potential temperature ($^{\circ}\text{C}$) (a), mixing ratio of water vapor (g kg^{-1}) (b), and U (solid) and V (dashed line) wind components (m s^{-1}) (c) for the baseline simulation based on the study by Leipper and Koraćin (1998). See above text for more details.

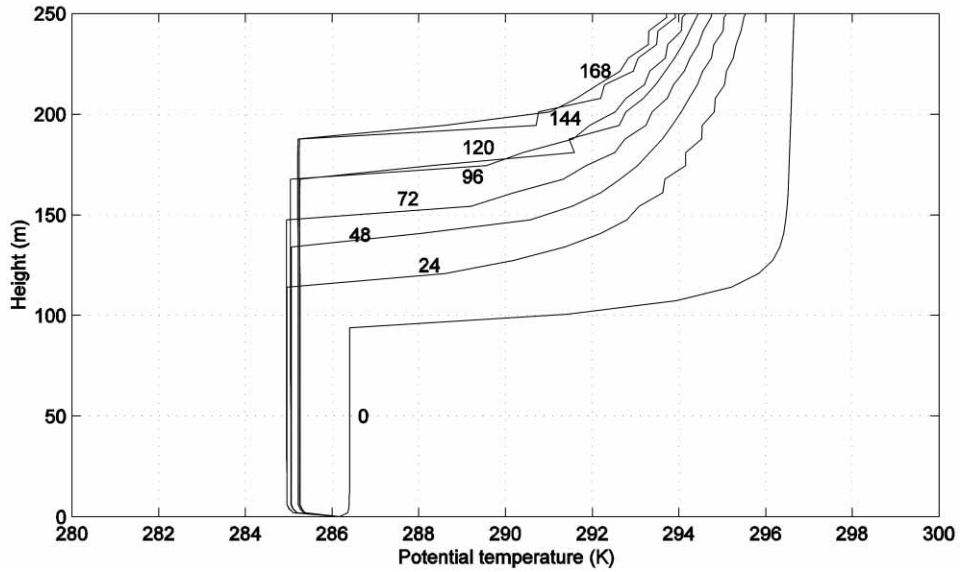


Figure 7. Evolution of the simulated potential temperature (K) profiles for the baseline simulation at various times after the simulation start.

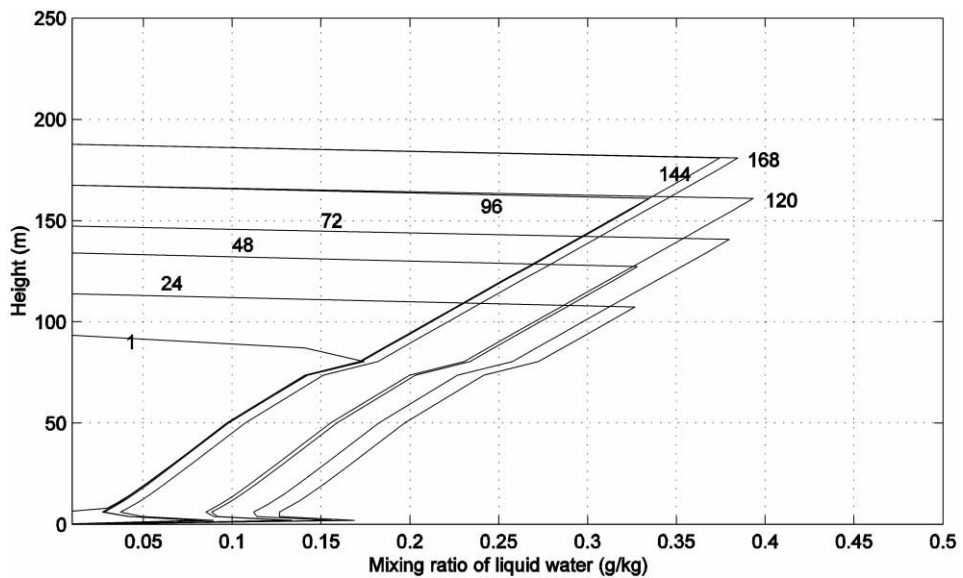


Figure 8. Evolution of the simulated profiles of the liquid water mixing ratio (g kg^{-1}) for the baseline simulation at various times after the simulation start.

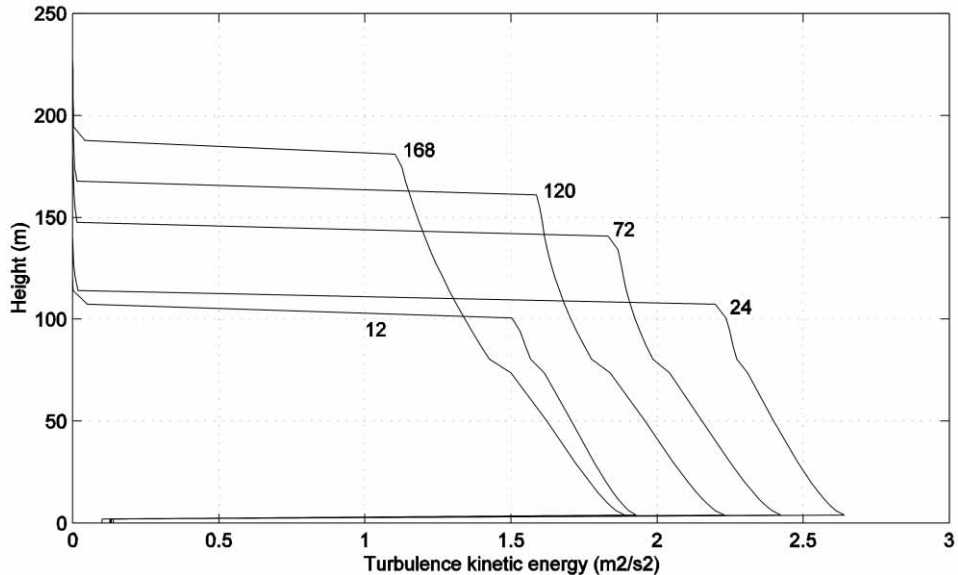


Figure 9. Vertical profiles of the simulated turbulence kinetic energy ($\text{m}^2 \text{s}^{-2}$) for selected hours after the simulation start.

4.2. Vertical resolution of the model grid

Vertical resolution of the model grid is always an important element in resolving physical processes. The increase in vertical resolution enables the prediction of a sharper temperature inversion, increased TKE, and a generally higher mixing ratio of liquid water. This is mainly a consequence of better representation of surface fluxes and radiation effects within the fog. We used 180 vertical points from the surface to 1200 m in the baseline simulation and all sensitivity tests. Since two- and three-dimensional models use much coarser vertical resolution, we also performed several tests with 45 and 90 vertical points. Simulations with coarser vertical grids revealed smoother gradients of the mean parameters near the surface and lower turbulence transfer as a consequence. Figure 10 shows a time series of the net radiative heating due to shortwave and longwave fluxes. The figure indicates that the coarse resolutions cannot resolve persistent and dominant fog-top cooling, and also that they overestimate the effect of shortwave heating. A weaker inversion was simulated, and longwave cooling at the fog top was reduced. Coarse vertical resolution affects longwave cooling more since this type of cooling is confined to the shallow layer at the fog top, while shortwave heating takes into account bulk properties of the fog layer and is therefore less affected by coarse resolution. The consequence is that shortwave heating becomes dominant and suppresses the overall cooling and destabilization of the

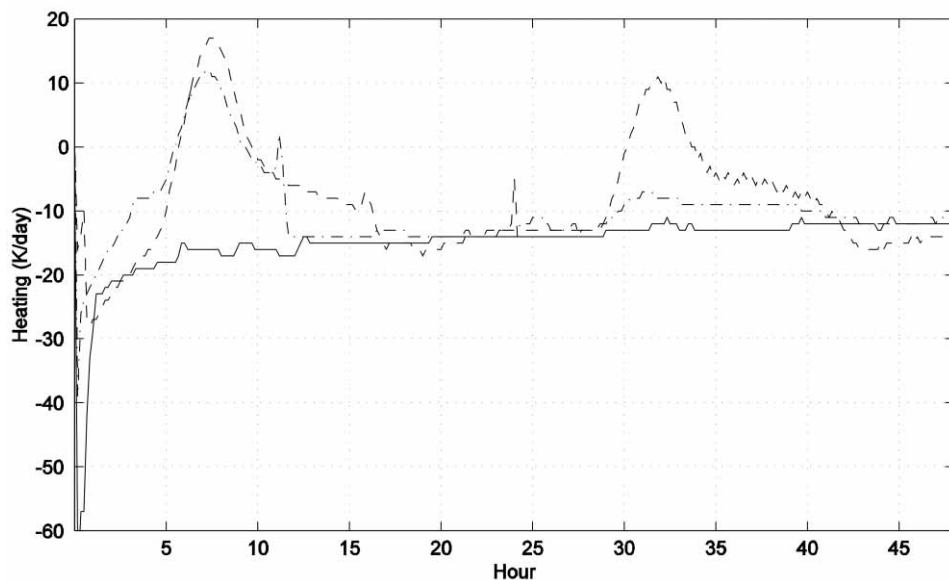


Figure 10. Time series of the simulated average net heating of the fog layer ($^{\circ}\text{C day}^{-1}$) due to longwave and shortwave radiative heat transfer for the baseline simulation with 180 vertical points (solid), the test run with 90 vertical points (dash-dot), and the test run with 45 vertical points (dashed line) within 1200 m.

fog layer by longwave cooling. The simulation results indicate that the coarser the grid, the greater the simulated net heating. This effect reduces the strength of the marine inversion and facilitates penetration of the fog layer into the hot-air layer. The mixed air is warmer, however, and the lifting condensation level is located at a higher elevation. In the simulation with the coarsest vertical resolution (45 points), the fog transforms into a stratus layer in the second part of the simulation time.

4.3. Sea-surface temperature

We performed two tests to investigate the effects of variable sea surface temperature on the formation and evolution of fog. In the first, the sea surface temperature was reduced by 2°C compared to the baseline. Thermodynamic conditions resulted in formation of fog within the entire near-surface layer within the first hour of the simulation. The fog layer was cooled by more than 3°C . Warming of the fog layer due to mixing with the hot-air layer was entirely neutralized by longwave radiative cooling at the fog top and a negative surface heat flux. The liquid water mixing ratio was reduced compared to the baseline simulation. Fog also grew as a mixed layer but at a slower rate than in the baseline run (Fig. 11).

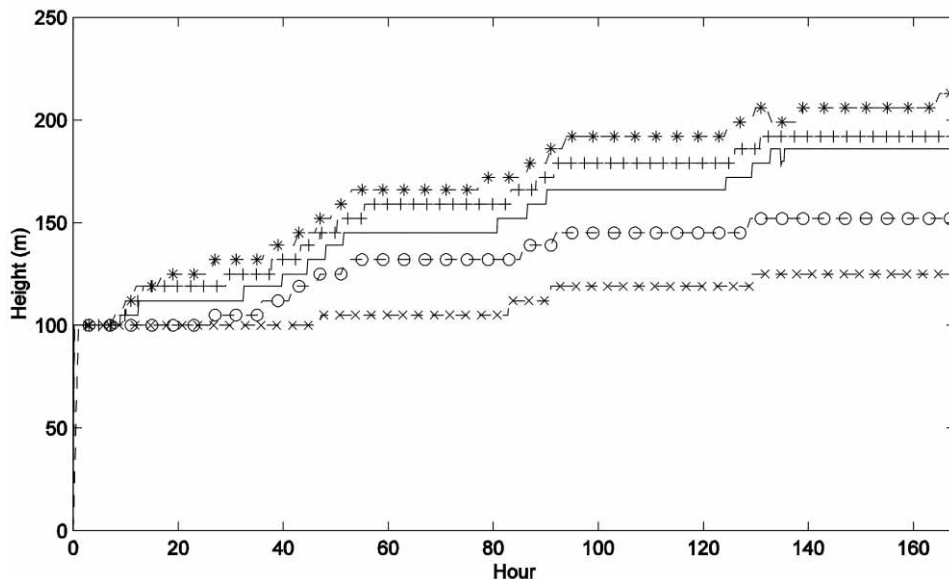


Figure 11. Evolution of the simulated fog top for the baseline run (solid line), a case with colder sea-surface temperature by 2 °C (o), a case with warmer sea-surface temperature by 2 °C as compared to the baseline run (*), a case with larger near-surface inversion (◊), and a case with a drier hot-air layer (+), as compared with the baseline run.

In the second test, the sea surface temperature was increased by 2 °C compared to the baseline. Thermodynamic conditions resulted in the formation of stratus clouds in the upper part of the near-surface layer within the first hour of the simulation. The mixed layer was cooled by only approximately 1 °C. Warming of the fog layer due to positive surface heat flux and mixing with the hot-air layer compensated for the longwave radiative cooling at the fog top. Positive surface moisture and heat fluxes generated more turbulent mixing than in the baseline simulation. The liquid water mixing ratio increased compared to the baseline run. Fog also grew as a mixed layer but faster than in the baseline and »cold sea surface« cases (Fig. 11).

4.4. Near-surface inversion stronger as compared to the baseline simulation

In his conceptual model of fog prediction, Leipper (1948, 1994, and 1995) emphasized that the existence of a strong near-surface inversion (generated by offshore flows and at least 5 °C or greater) is an essential condition for the formation and evolution of coastal fog. To gain further insight, we increased the near-surface inversion strength from 10 to 15 °C. Fog formed initially and grew as a mixed layer. The rate of growth, however, was slower than in the baseline simulation (Fig. 11). The fog top reached a quasi-equilibrium height

of 127 m during the seventh day of this simulation. This reduced growth is a consequence of the available TKE which was not sufficient to grow the boundary layer against the capping strong inversion. The maximum liquid water mixing ratio was reduced by approximately 0.1 g kg^{-1} compared to the baseline simulation since the mixing included warmer air above the fog.

4.5. Hot-air layer drier than in the baseline simulation

In order to investigate whether the dryness of the hot-air layer would influence the evolution of fog, we simulated an initial mixing ratio of water vapor decrease of 7 g kg^{-1} from the hot-air layer to the top of the domain, compared to a decrease of 5 g kg^{-1} in the same layer in the baseline simulation. The drier layer overlying the fog facilitated increased longwave radiative cooling and consequent turbulent mixing within the fog layer. Additional energy for mixing and fog growth was provided by evaporative cooling during the mixing between the saturated marine air and the dry hot-air layer. The boundary layer grew at a faster rate compared to the baseline case (Fig. 11). The simulated integrated liquid water content was greater than in the baseline simulation (Fig. 12). Stronger fog-top cooling generates turbulence that increases vertical transport of moisture. This effect was partially reduced at the end of simulation due to increased mixing of the deeper fog with the hot and dry layer.

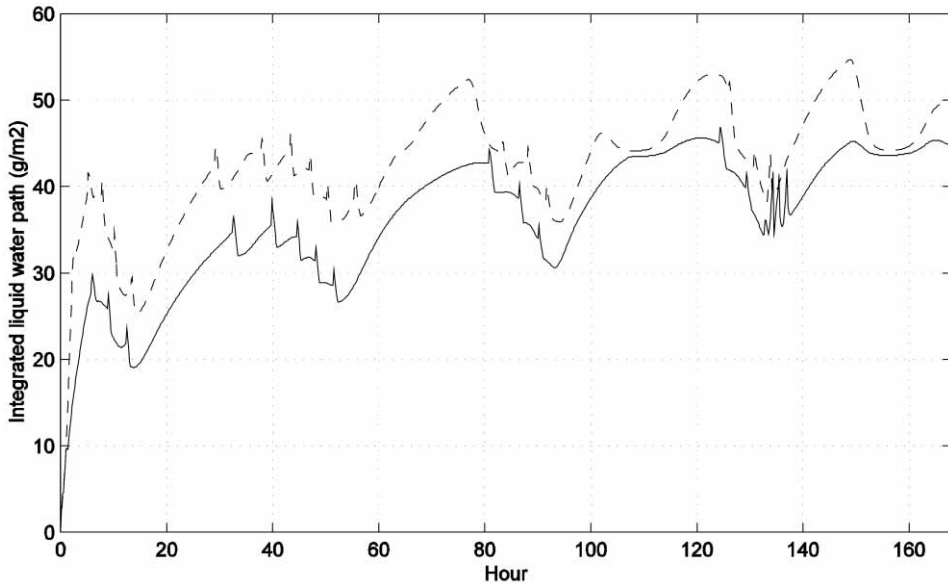


Figure 12. Integrated liquid water path (g m^{-2}) for the baseline run with a decrease in the initial mixing ratio of water vapor of 5 g kg^{-1} from the top of the near-surface layer up to the model top (solid), and a case with a larger decrease in the initial mixing ratio of water vapor of 7 g kg^{-1} (dashed line).

4.6. Random perturbations in the surface wind speed

Due to the inability of the model to treat surface ocean waves and their effects on perturbation of airflow at the lowest levels, we performed a test in which the wind field was perturbed at the initial stage of the simulation. Within the first hour, the U and V wind velocity components at the first twelve levels were perturbed by a random component ranging from -1 to 1 m s^{-1} . This perturbation, in principle, can provide a short-term source of energy for additional mixing within the near-surface layer. This energy can facilitate penetration of the near-surface marine layer into the hot-air layer and associated mixing. Figure 13 shows that the fog grew initially at a faster rate than in the baseline simulation. The greatest effect of the perturbed wind components within the first hour extended into the next few hours. An increased integrated liquid water path was simulated during the entire first day; however, this influence decayed with time as the turbulence redistributed the perturbations.

5. Conceptual model of sea fog initiated by a hot spell

Results from the numerical experiment clearly indicate the complexity of the physical processes that govern the formation and evolution of sea fog on the U.S. California coast. Both Leipper's conceptual model (Leipper, 1948;

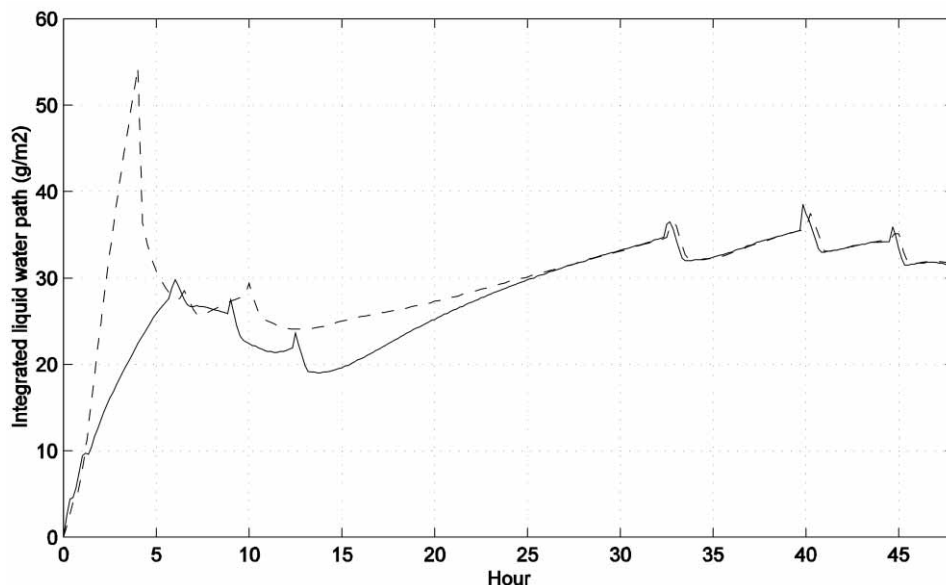


Figure 13. Integrated liquid water path (g m^{-2}) for the baseline run (solid), and a case with perturbed wind components in the near-surface layer (dashed line) (see text).

1994; and 1995) and the present simulations confirm a scenario of coastal fog formation and growth during hot spells (warm and dry offshore flow events). It has been observed that these warm/hot and dry offshore flows generally precede the occurrence of fog. This pattern can last for several days, and in addition to subsidence the warm and dry air efficiently lowers the marine inversion near the surface. The displacement and spreading of the high-pressure system over the land in our case study induced offshore flows and increased subsidence that strengthened the inversion and initiated extensive cloud clearing offshore. Weak pressure gradients at the surface induced weak winds, and stable stratification reduced the turbulence kinetic energy. Subsidence overpowered the weak turbulence kinetic energy and significantly reduced the depth of the marine layer, which became confined into a very shallow, near-surface region. Moisture is then capped by this near-surface inversion. A warm and dry air layer overlying the moist and cool marine layer induces enhanced radiative cooling at the top of the marine layer and promotes saturation. The relatively small but negative heat flux associated with upwelled and cool coastal waters also facilitates condensation and formation of fog. Once the saturated layer is formed, it generates cooling and turbulence, propagates downward, and eventually fog forms in the entire thin marine layer.

The coupling between radiative and turbulence processes becomes the dominant process in fog evolution. Consequently, the fog grows as a mixed layer and the marine inversion rises. Longwave radiative cooling at the fog top is one of the principal generators of turbulent mixing and penetration of the fog into the hot-air layer. As the fog grows, the mixed layer can become colder than the sea surface due to fog-top radiative cooling. Radiative cooling is enhanced due to the significant dryness of the hot-air layer characterized by the large moisture drop at the base of the hot-air layer (the base of the inversion). Subsequent mixing of the fog layer with the hot and dry layer above results in heating of the mixed layer with a reduction in liquid water. Among other parameters, the dryness of the hot-air layer determines the degree of longwave cooling initiated at the interface between these layers. Evaporative cooling during the mixing between the near-surface, saturated layer and the dry, hot-air layer contributes to enhanced fog growth. An increase in the inversion strength also results in the formation of fog; in that case, the fog growth is much slower. The simulations also indicated that fog could be formed in similar conditions over relatively warm water.

6. Concluding remarks

This study is a first step in investigating the roles of thermodynamical, dynamical, radiative, and turbulence processes in the formation and evolution of sea fog in coastal regions during hot spell events. Based on the numerical experiment, the study offers an explanation of the formation of sea fog under offshore warm advection that efficiently lowers the marine layer inver-

sion and confines the moisture to a very shallow layer. Longwave radiative cooling of the marine layer top is enhanced due to the dryness and high temperature of the overlying hot-air layer and eventually leads to saturation at the marine-layer top. Intense longwave cooling of the saturated layer generates cooling and turbulence within the marine layer that triggers saturation of the entire shallow layer as sea fog. Fog grows as a mixed layer and in some cases becomes colder than the surface. The entrainment of the warm layer from above the inversion during the fog growth and increased surface heat flux (fog colder than the surface) acts to dissipate the fog and eventually lift it into the stratus. Consequently, all of the relevant processes – the synoptic forcing, balance among surface fluxes, radiation, turbulence, and the properties of the marine layer and overlying hot-air layer – will determine fog evolution, maintenance, and dissipation.

A series of sensitivity tests was performed to examine the roles and interplay of the main physical processes, initial and boundary conditions, and model setup parameters on sea fog formation and evolution. High vertical resolution (180 points) appears to be crucial to resolving thermodynamical, dynamical, and especially radiative effects near the surface, within the fog, and in the inversion layer. Coarser resolution (45 points) implies weaker gradients, and consequently the radiative fluxes and turbulence parameters are not adequately calculated. Coarse vertical resolution significantly alters the estimate of longwave fluxes at the cloud top while the estimate of shortwave radiative transfer, which is usually obtained from bulk cloud properties, is less affected. Simulations with coarser grids overestimated heating in the upper and lower portions of the fog compared to the higher-resolution simulations. This effect resulted in dissipation of the fog near the surface and its transformation into stratus. Also, cooling is maintained within the stratus layer as the longwave cooling maximum becomes further distant from the shortwave heating maximum. In coarser-resolution simulations, a large thermal inversion is created at the stratus base, and the stratus is decoupled from the subcloud layer with respect to turbulence structure. More details on the decoupling process that can significantly influence the fate of the fog/stratus layer are discussed in studies by Nicholls (1984), Koračin and Rogers (1990), Rogers and Koračin (1992), and Tjernström and Koračin (1995), among others. It is important to note that in some cases the selection of vertical resolution can dictate the fate of simulated fog or stratus formation and evolution. A decrease in the SST induces increased cooling of the entire fog layer as well as greater stability and reduced turbulence within the near-surface layer. In this study, higher SST than in the baseline run resulted in more intense growth of the fog. The main reason is that increased surface heat and moisture fluxes generate higher turbulent transfer and consequent growth. This effect could be important in explaining fog occurrence over relatively warm water such as on the southern California coast, as discussed by Petterssen (1938). If the heat flux becomes too great, however, the lifting condensation

level will be above the near-surface layer, and fog will not occur. In some cases, fog may form over a cool water region and grow at a relatively slow rate. If it then drifts toward a relatively warm sea surface, growth will be enhanced.

A stronger thermal inversion than in the baseline run also resulted in fog formation, but the fog growth was at a slower rate. The same amount of generated turbulence is not sufficient to maintain the same depth of the boundary layer as that capped by the weaker inversion.

The knowledge gained from this and other fog studies should be used as a guide in setting up initial and boundary conditions as well as appropriate treatment of physical processes in two- and three-dimensional simulation studies. Further investigation of hot-spell events is needed for better understanding of fog formation and evolution. Detailed measurements prior to fog formation and during its growth are essential to shedding more light on this phenomenon. The data to be collected over the ocean in the future should be used both to test conceptual models and to evaluate numerical models.

Acknowledgments – This study was supported by the Department of Defense, Office of Naval Research, Marine Meteorology and Atmospheric Effects, grants N00014-96-1-0980 and N00014-96-1-1235. The authors (DK and JL) owe gratitude to the late Dr. Dale Leipper of the Desert Research Institute who died prior to the completion of this study (Obituary, 2004). He provided great inspiration, valuable discussions, comments, and encouragement in conducting the study as well as motivation for sea fog research. Inspiring discussions and valuable comments were provided by Dr. Clive Dorman of the Scripps Institution of Oceanography, San Diego, CA, U.S.A. and Dr. Joost Businger of the University of Washington, Seattle, WA, U.S.A. The author thanks Mr. Travis McCord and Mr. Domagoj Podnar for help in the technical preparation of the manuscript.

References

- Beg Paklar, G., Isakov, V., Koračin, D., Kourafalou, V. and Orlić, M. (2001): A case study of bora-driven flow and density changes on the Adriatic shelf (January 1987). *Cont. Shelf Res.*, **21**, 1751–1783.
- Burk, S. D. and Thompson, W. T. (1992): Airmass modification over the Gulf of Mexico: Mesoscale model and airmass transformation model forecasts. *J. Appl. Meteorol.*, **31**, 925–937.
- Filonczuk, M. K., Cayan, D. R. and Riddle, L. G. (1995): Variability of Marine Fog along the California Coast. Report 95–2, Scripps Institution of Oceanography, La Jolla, CA, 92093–0224, 91 pp.
- Hsu, S. A. (1988): *Coastal Meteorology*. Academic Press, Inc., San Diego, CA. 260 pp.
- Koračin, D. (1989): Numerical simulations of the cloud-capped marine boundary layer. Ph.D. Dissertation. University of Nevada, Reno, 151 pp.
- Koračin, D. and Rogers, D. P. (1990): Numerical simulations of the response of the marine atmosphere to ocean forcing. *J. Atmos. Sci.*, **47**, 592–611.
- Koračin, D. and Dorman, C. E. (2001): Marine atmospheric boundary layer divergence and clouds along California in June 1996. *Mon. Weather Rev.*, **129**, 2040–2055.
- Koračin, D., Dorman, C. E. and Dever, E. P. (2004): Coastal perturbations of marine layer winds, wind stress, and wind stress curl along California and Baja California in June 1999. *J. Phys. Oceanogr.*, **34**, 1152–1173.

- Koraćin, D., Businger, J. A., Dorman, C. E. and Lewis, J. (2005): Formation, evolution, and dissipation of coastal sea fog. *Bound-Lay. Meteorol.* (in print).
- Koraćin, D., Lewis, J., Thompson, W. T., Dorman, C. E. and Businger, J. A. (2001): Transition of stratus into fog along the California coast: Observations and modeling. *J. Atmos. Sci.*, **58**, 1714–1731.
- Leipper, D. F. (1948): Fog Development at San Diego, California. *J. Mar. Res.* (Sears Foundation) **VII**(3), 337–346.
- Leipper, D. F. (1994): Fog on the U.S. West Coast, a review. *B. Am. Meteorol. Soc.*, **72**, 229–240.
- Leipper, D. F. (1995): Fog forecasting objectively in the California coastal area using LIBS. *Weather Forecast.*, **10**, 741–762.
- Leipper, D. F. and Koraćin, D. (1998): Hot spells and their role in forecasting weather events on the U.S. west coast. In *Proceedings of the Second conference on coastal and oceanic prediction and processes*, 11–16 January 1998, Phoenix, Arizona, U.S., 127–132.
- Lewis, J., Koraćin, D., Rabin, R. and Businger, J. (2003): Sea fog off the California coast: Viewed in the context of transient weather systems. *J. Geophys. Res.-Atmos.*, **108**, No. D15, 4457, 10.1029/2002JD002833.
- Lewis, J., Koraćin, D. and Redmond, K. (2004): Sea fog research in the UK and USA: Historical essay including outlook. *B. Am. Meteorol. Soc.*, **85**, 395–408.
- Nicholls, S. (1984): The dynamics of stratocumulus: Aircraft observations and comparison with a mixed layer model. *Q. J. Roy. Meteorol. Soc.*, **110**, 783–820.
- Nuss, W. A., Bane, J. M., Thompson, W., Dorman, C. E., Ralph, F. M., Rotunno, R., Klemp, J., Skamarock, W., Samelson, R., Rogerson, A., Reason, C. and Jackson, P. (2000): Coastally trapped wind reversals: Progress toward understanding. *B. Am. Meteorol. Soc.*, **81**, 719–743.
- Obituary (2004): Dale F. Leipper. *B. Am. Meteorol. Soc.*, **85**, 769–770.
- Oliver, D. A., Lewellen, W. S. and Williamson, G. G. (1978): The interaction between turbulent and radiative transport in the development of fog and low-level stratus. *J. Atmos. Sci.*, **35**, 301–316.
- Petterssen, S. V. (1938): On the causes and forecasting of the California fog. *B. Am. Meteorol. Soc.*, **19**, 49–55.
- Pilić, R. J., Mack, E. J., Rogers, C. W., Katz, U. and Kocmond, W. C. (1979): The formation of marine fog and the development of fog-stratus systems along the California coast. *J. Appl. Meteorol.*, **18**, 1275–1286.
- Rogers, D. P. and Koraćin, D. (1992): Radiative transfer and turbulence in the cloud-topped marine atmospheric boundary layer. *J. Atmos. Sci.*, **49**, 1473–1486.
- Rosenthal, J. (1974): Some applications of satellite imagery to Naval Test and Evaluation. Block Program ZF52–551–001, Geophysics Division, Pacific Missile Test Center, Point Mugu, California, PMTC–TP–78–4, September, 50–61.
- Smith, W. S. and Kao, C.-Y. J. (1996): Numerical simulations of observed Arctic stratus clouds using a second-order turbulence closure model. *J. Appl. Meteorol.*, **35**, 47–59.
- Stage, S. A. and Businger, J. A. (1981): A model for entrainment into a cloud-topped marine boundary-layer. Part I: Model description and application to a cold-air outbreak episode. *J. Atmos. Sci.*, **38**, 2213–2229.
- Tjernström, M. and Koraćin, D. (1995): Modeling the impact of marine stratocumulus on the boundary-layer structure. *J. Atmos. Sci.*, **52**, 863–878.

SAŽETAK

**Modeliranje magle nad morem na obali Kalifornije u slučaju
»Vruće Kaplje«**

Darko Koračin, Dale F. Leipper i John M. Lewis

Pojava magle na moru uzduž američko-pacifičke obale je često povezana s promjesticanjem istočno-pacifičke anticiklone na kopno. U tom slučaju prisutno je višednevno zagrijavanje kopna i razvoj »vruće kaplje« (»hot spell«) te vjetrova koji pušu s kopna na more neposredno prije pojave magle. Cilj ove studije je modeliranje stvaranja i razvoja magle na moru kao posljedice interakcije vrućeg i suhog vjetera s kopna i hladnog i vlažnog maritimnog graničnog sloja. Simulacije potvrđuju izloženi temeljni teorijski model formiranja i razvoja magle nad morem koji je temeljen na fizikalnim procesima u kojima vjetrovi s kopna spuštaju maritimnu inverziju neposredno do morske površine. Uprkos advekciji suhog i toplog zraka, magla nad morem nastaje u plitkom površinskom sloju koji je zatvoren s gornje strane s inverzijom od 10 °C(K) ili više te slojem vrućeg zraka iznad inverzije. Prije formiranja magle na moru, negativni površinski senzibilni fluks topline uzrokuje hlađenje i kondenzaciju dok latentni toplinski fluks doprinosi povećanju vlage i turbulencije u površinskom sloju. Suhoća toplog sloja zraka nad maritimnim slojem uzrokuje pojačano dugovalno radijacijsko ohlađivanje na vrhu maritimnog sloja i pospješava kondenzaciju. Isprva se formira tanki oblak koji se ubrzano razvija prema površini mora te se pretvara u maglu nad morem. Čim se magla formira, radijacijsko ohlađivanje gornje granice stvara turbulentna gibanja i razvoj magle kao sloj miješanja. Uslijed radijacijskog ohlađivanja, magla postaje u početku hladnija od površine. U kasnijoj fazi razvoja magle, stalno miješanje hladnog i vlažnog maritimnog zraka s toplim i suhim slojem iznad inverzije ograničava turbulentno miješanje. Uslijed toga podiže se visina kondenzacijskog nivoa te dolazi do razbijanja magle ili njezine transformacije u stratus.

Ključne riječi: Interakcija zrak-more, dugovalno radijacijsko ohlađivanje, maritimni atmosferski granični sloj, numeričke simulacije, vjetrovi koji pušu s kopna na more, obalna magla, zapadna obala SAD-a

Corresponding author's address: Darko Koračin, Desert Research Institute, 2215 Raggio Parkway, Reno, NV, U.S. 89512; e-mail: Darko.Koracin@dri.edu; tel: ++1 (775) 674-7091; fax: ++1 (775) 674-7060.